

Senior Research

Performance Analysis of the Invariant
Algorithm for Target Detection in
Hyperspectral Imagery

Final Report

Rachael Gold
Center for Imaging Science
Rochester Institute of Technology
May 2005

Copyright © 2005
Center for Imaging Science
Rochester Institute of Technology
Rochester, NY 14623-5604

This work is copyrighted and may not be reproduced in whole or part without permission of the Center for Imaging Science at the Rochester Institute of Technology.

This report is accepted in partial fulfillment of the requirements of the course 1051-503 Senior Research.

Title: Performance Analysis of the Invariant Algorithm for Target Detection in Hyperspectral Imagery
Author: Rachael Gold
Project Advisor: David Messinger
1051503 Instructor: Joseph P. Hornak

Performance Analysis of the Invariant Algorithm for Target Detection in Hyperspectral Imagery

Rachael Gold

Center for Imaging Science
Rochester Institute of Technology
Rochester, NY 14623-5604

5/20/05

Abstract

Hyperspectral imaging is one of the principal new breakthroughs in the field of remote sensing. As opposed to multispectral data, hyperspectral data, which contains hundreds of contiguous spectral bands, allows for a more accurate spectral signature to be recognized using various target detection methods for satellite and airborne sensors. All of these target detection routines involve compensating for the effects of calibration and atmosphere. While this is successful for high contrast targets imaged in well-behaved atmospheric conditions with even, reliable illumination conditions, this clearly is not always the case. For more complicated situations, one can not simply compensate for the atmospheric and illumination conditions by taking them out. The Invariant Algorithm for target detection was designed to find many possible combinations of these conditions for the image. With this method, one may find all possibilities of how the target may appear spectrally.

The Digital Imaging and Remote Sensing group at the Rochester Institute of Technology has implemented a version of the Invariant Algorithm for target detection. The Invariant Algorithm has proven to work for uncontaminated targets (i.e. clean targets) [1]. This work exercises and optimizes the algorithm for a number of target types and obscuring conditions. Data analyzed were from the 2004 MegaCollect using MISI and COMPASS for targets contaminated with dirt as well as those under camouflage and tree canopies. The Invariant Algorithm, after preliminary analysis, shows some effectiveness at addressing this class of targets.

Acknowledgements

I would like to thank my advisor, David Messinger, for all of his help in understanding and completing this project. I never could have pulled off this task without his ever-patient advice and assistance.

I would also like to thank Sue Chan for convincing my parents that this major was a good choice. I never would have made it through these last four years without her guidance and sincere hope for my wellbeing.

Last but not least, I would like to thank my parents for giving me all of the opportunities that I've been able to experience. I know that without both of you, none of this would have been possible.

Table of Contents

Abstract	ii
Acknowledgements	iii
Table of Contents	iv
Introduction	1
Background.....	2
Experimental Methods	6
Results.....	10
Conclusions & Future Work.....	21
References	23
Appendix.....	24

Introduction

In the field of Remote Sensing, few topics are as important as target detection. The theory behind target detection is fairly simple. Each object has a unique spectral signature that can be measured in lab under predictable conditions. A hyperspectral sensor measures spectral curves in unpredictable conditions caused by changes in illumination and atmosphere. Most target detection algorithms attempt to remove the illumination and atmospheric conditions from the sensor measured spectrum to make it look like a lab measured spectrum. This form of target detection is very successful for high contrast targets imaged in well-behaved atmospheric conditions. Because of the irregularity of these conditions, this proves to be a difficult task at times [2]. A new method for target detection was created to overcome these difficulties. The method is intended to be “invariant” to the variable illumination conditions and is therefore termed the Invariant Algorithm. This method for hyperspectral target detection will be described in greater detail in the following sections [3].

The Invariant Algorithm is a fairly recent development, and as such, its small faults and errors have yet to be found. This research was performed to characterize the performance of the Invariant Algorithm for two different data sets, one with clean targets and one with contaminated and concealed targets. The study was created to determine how to maximize the target pixel probability by completing a parameterization study for each set of data. The conclusions drawn from this experiment will be useful for further research in contaminated and concealed target detection, and for the further development of the Invariant Algorithm for target detection.

Background

Hyperspectral sensors measure the radiance of an object at a very large number of contiguous spectral wavelength bands. The fact that these sensors use such a large number of wavelength bands allows scientists to more accurately classify a pixel by comparing the measured radiance curve with similar known curves from a spectral library. In other words, the use of optical properties is implemented, as opposed to the use of spatial properties. Generally, target detection involves the use of “spectral matched filters” in the reflectance domain [2]. Hyperspectral images taken overhead (using satellite or airborne sensors) need to be compensated for the effects of calibration and atmosphere [3]. The following equation is used to calculate the calibrated radiance data:

$$L(\lambda) = (E_0(\lambda)\cos\theta + L_d(\lambda))\rho(\lambda)\tau_{atm}(\lambda) + L_u(\lambda) \quad (1)$$

where $L(\lambda)$ is the at-sensor radiance, $E_0(\lambda)\cos\theta$ is the solar illumination for a particular pixel, $L_{d,u}(\lambda)$ are the downwelling and upwelling atmospheric radiances, $\tau_{atm}(\lambda)$ is the atmospheric transmission, and $\rho(\lambda)$ is the surface target reflectance. The Invariant Algorithm was created to be invariant to illuminations that can not be accounted for in the typical target detection algorithm. This new algorithm finds every possible combination of the atmospheric and illumination conditions for the image, since these are generally not known. Listing every possible combination of these conditions would clearly be too long to manage, so ground truth data is used to narrow down the list. Ground truth parameters, such as latitude, longitude, time of day, and time of year can all be used to constrain the possible conditions. By constructing this inventory of various atmospheric possibilities, it is possible to develop the same number of possible ways that the target may manifest itself in the scene [3]. This way, the atmospheric and illumination variations can be normalized out of the detection process.

The Invariant Algorithm involves considering each pixel as the sum of a target subspace vector, a background subspace vector, and a noise vector. The target subspace contains target material information of illumination and atmospheric conditions. The background subspace contains spectral information about other materials in a region of the scene. This data is used to compute a probability map that shows the likelihood that the target is present at each pixel in an image [4]. The probability map is thresholded, and the pixels with likelihoods above the thresholds are considered targets.

The target subspace is this set of possible ways in which the target may appear in a scene. This is a vector space whose dimensionality is the number of spectral bands in the image (which is of course determined by which sensor is used). The Center for Imaging Science’s MaxD program (created to implement the Invariant Algorithm for target detection) finds the initial number of basis vectors, and then reduces that set through forward step-wise regression to a single set of basis vectors that spans the target space.

Next, the background subspace is constructed. Again, this subspace is the space that is spanned by the background component spectra. Every pixel in the image is treated as a vector

in the background space. The MaxD program is used to reduce the space to a set of background basis vectors. Once this is completed, every pixel in the image is modeled with both the set of target basis vectors and the set of background basis vectors, creating target models and background models. The detection is based on a GLRT (generalized likelihood ratio test). Basically, this means that the value of the probability is found by comparing how much the spectrum of the pixel in question looks like the target spectrum to how much it looks like the background pixel. If the target model created by the target basis vectors more accurately matches the pixel in question than the background model created by the background basis vectors, then the pixel has a higher probability of being a target [3]. A probability map is created, which estimates the likelihood that each pixel is target material. A threshold is applied, and the pixels with high enough probabilities are considered targets. This entire process can be seen visually in Figure 1 below.

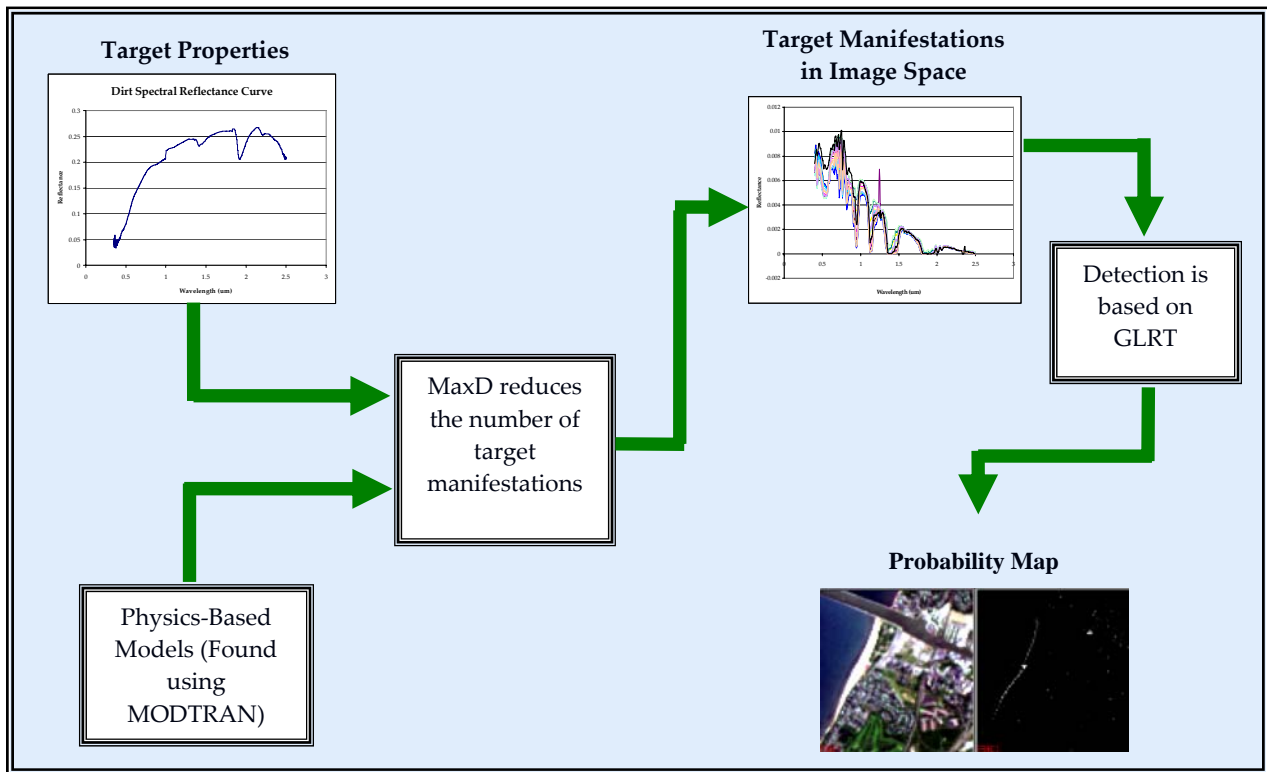


Figure 1: Flowchart representing the process of the Invariant Algorithm.

The MaxD program has been successfully applied to hyperspectral AVIRIS data. AVIRIS (the Airborne Visible/Infrared Imaging Spectrometer) is a 224 channel hyperspectral sensor with wavelengths ranging from 400-2500 nanometers. The Invariant Algorithm was applied to a set of AVIRIS data (displayed in Figure 2(a)). The target was the red basketball court shown in Figure 2(b). The results for this study were positive. Any mismatched pixel could be attributed to three variables: the pixel was not fully mixed, the measured reflectance spectrum was not a true representation of the actual surface, or the parameters used to model the atmosphere in the image were slightly off [1]. The probability map that was created can be

seen in Figure 3 (a). By implementing a threshold, Figure 3(b) is created. This is the probability map that is formed after the threshold has been applied. It shows the pixels that are detected as target pixels (in this case, basketball court pixels).

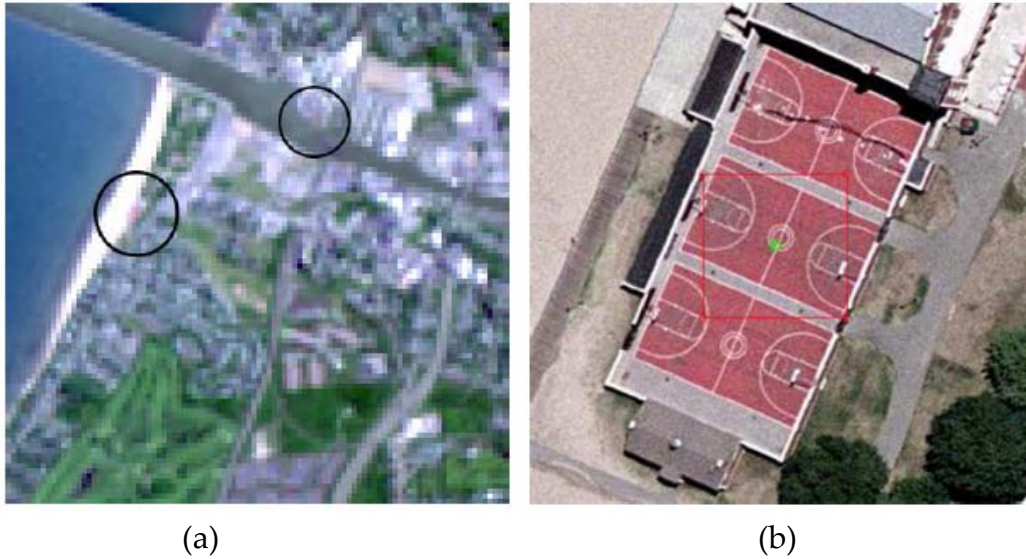


Figure 2: (a) AVIRIS 100 x 100 image. Bands 9, 19, and 29 are displayed. Two regions, containing interesting targets, are circled. The region on the left contains a red basketball court while the region on the right contains a red tennis court. (b) High resolution of the red basketball court is shown. An AVIRIS pixel is drawn over the court to indicate its size relative to the high-resolution imagery [1].

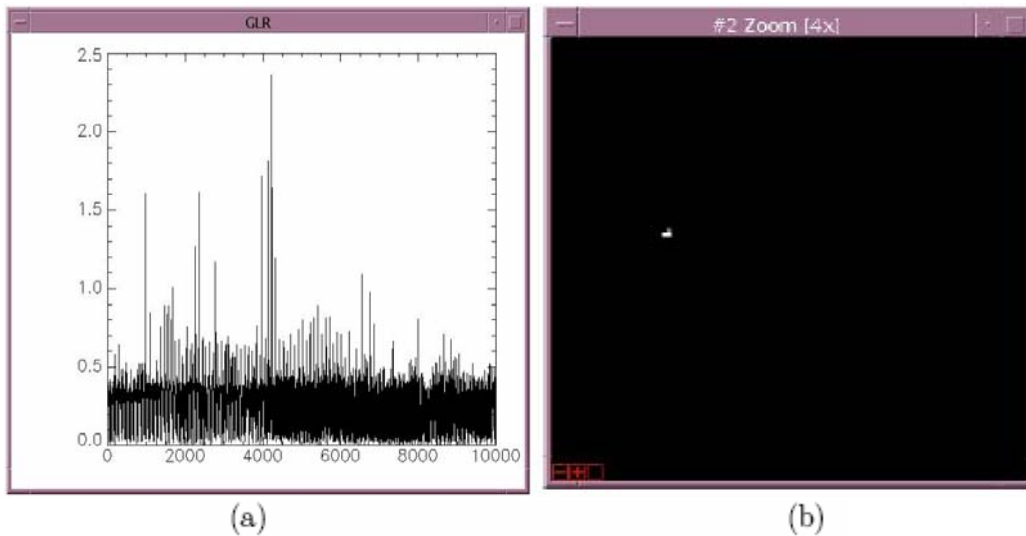


Figure 3: (a) This shows the probability map formed from the AVIRIS data being run through MaxD. The x-axis is pixel number while the y-axis is proportional to a probability of detection. This shows the target detection probability map. Implementing a threshold illustrates that the 3 three highest-valued pixels are of the basketball court [1]. (b) This shows the target detection probability map. When figure (a) is thresholded, these are the three pixels that are detected as being the basketball court.

The first part of the research was to perform a parametric sensitivity study. This study aided in the elimination of the third possible error when detecting target pixels. The MaxD

program has many parameters that can be modified, including the number of target basis vectors, the number of background basis vectors, and the detection threshold, among other things. Better results (fewer false alarms) may be achieved by adjusting the parameters.

The second part of the study involved running images containing contaminated and concealed targets through MaxD, in order to test if the Invariant Algorithm is successful for these obstacles. A contaminated target has surface contaminants covering it, such as dirt. A concealed target is partially obscured, as if covered by a tree for instance. Previously, the algorithm had only been run for uncontaminated, unconcealed targets, such as the AVIRIS image shown in Figure 2(a). The second goal in the experiment was to determine whether or not the current algorithm would work successfully with contaminated and concealed data. In the long run, being able to detect concealed and contaminated targets using spectral data will become especially significant. If this algorithm proves to work for a white tarp covered with dirt or a camouflage net, it could be applied to more useful functions.

The hypothesis of this study was to determine whether or not the MaxD program, an ENVI program created by the Digital Imaging and Remote Sensing group, would be able to detect contaminated or concealed target data using the Invariant Algorithm. The main goal of the experiment was to characterize the performance of the algorithm for a new data set, which includes contaminated and concealed targets

Experimental Methods

Many steps were taken in order to characterize the performance of the Invariant Algorithm, and to answer the question of whether or not the MaxD program will be able to detect contaminated target data using the Invariant Algorithm. Previously, the MaxD program had applied to a set of AVIRIS data (displayed in Figure 2(a)). The target was the red basketball court shown in Figure 2(b). The results for this study were positive. Any mismatched pixel could be attributed to three variables: the pixel was not fully mixed, the measured reflectance spectrum was not a true representation of the actual surface, or the parameters used to model the atmosphere in the image were slightly off [1]. The probability maps that were created can be seen in Figures 3(a) and 3 (b).

The first step in the process of testing the hypothesis was to rerun the AVIRIS data with the uncontaminated targets, in order to ensure that the results can be easily duplicated. The procedure for implementing the MaxD program has been documented [1]. This method was executed for the same AVIRIS data that had been previously run. If the results of the study could be duplicated, the next part of the study would be initiated. If these results could not be duplicated, the MaxD program would be revised until it runs correctly. Once the probability maps shown in Figures 3(a) and 3(b) were reproduced, the next part of the study would begin.

This past summer, the Digital Imaging and Remote Sensing group, in collaboration with the National Geospatial-Intelligence Agency (NGA), supported a day of collecting data from the Megascene 1 area, a region of land in Rochester, NY. The goal of these Megascene collects is to collect near-simultaneous data over the whole scene, including ground truth, weather data, and hyperspectral data from multiple airborne and satellite sensors [5]. Six sensors were used in the collect that occurred June 7th, 2004. Out of these six, the procedure for this research project will include two sensors. The first is the COMPASS sensor (the Compact Airborne Spectral Sensor), an airplane-mounted 384 band hyperspectral sensor ranging from 400 to 2350 nm [5]. The second sensor is Rochester Institute of Technology's MISI sensor (Modular Imaging Spectrometer Instrument), a 72 channel spectrometer. It covers 400 to 1020 nm in increments of 10 nm [7]. Figures 4(a) and 4(b) show images of both the COMPASS sensor and the MISI sensor.

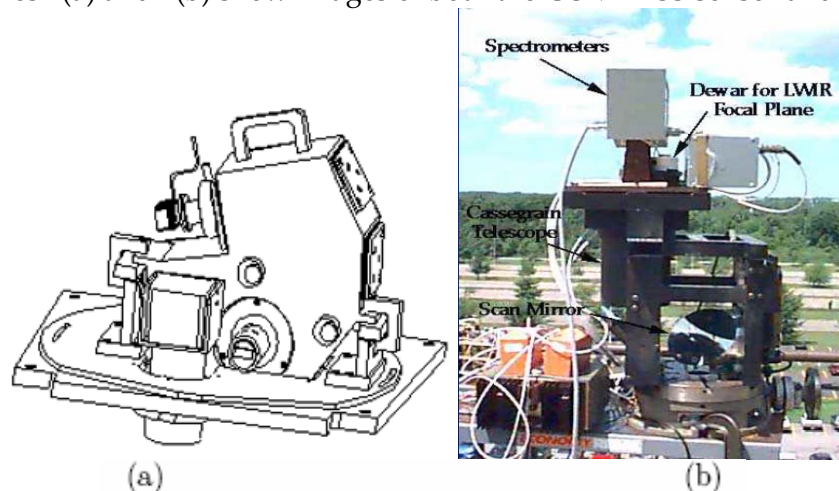


Figure 4: (a) A drawing of the COMPASS sensor [7] and (b) an image of the MISI sensor [6].

On June 7th, 2004, the Megascene collect (also called the Megacollect) was successfully conducted. Many different targets were used, including uncontaminated targets, contaminated targets, and concealed targets. Generally, these targets were all black, white, and gray tarps. Ground truth was taken for each sample taken, including GPS (Global Positioning System, a system for determining position on the Earth's surface by comparing radio signals from several satellites) location, the surface-leaving radiance, the reflectance (including that of the targets, contaminants, and the surround), and the temperature. Photographs were taken of every target [5].

The contaminated targets were covered with a layer of dirt or leaves. The concealed targets were placed underneath trees, in order to make them partially obscured. The images of these targets (taken for ground truth data) can be seen in Figures 5(a) and 5(b). A second type of concealed target was tested. This target can be seen in Figures 5(c) and 5(d). The target is covered with a camouflage net. One of the long term goals of this project would be to enable the military to find objects concealed by camouflage nets. Performing this target detection experiment would allow researchers to figure out whether or not the Invariant Algorithm works for objects concealed by these nets.



(a)



(b)



(c)



(d)

Figure 5: (a) Contaminated target (covered in leaves). (b) Concealed target (partially obscured by trees). (c) Target concealed by camouflage net. (d) Close up of target concealed by a camouflage net [5].

All of the data for these targets was collected during the Megacollect. Hyperspectral images were taken of the sites containing these targets. These images can be represented in a type of data cube. An example of this can be seen in Figure 6. This figure shows the

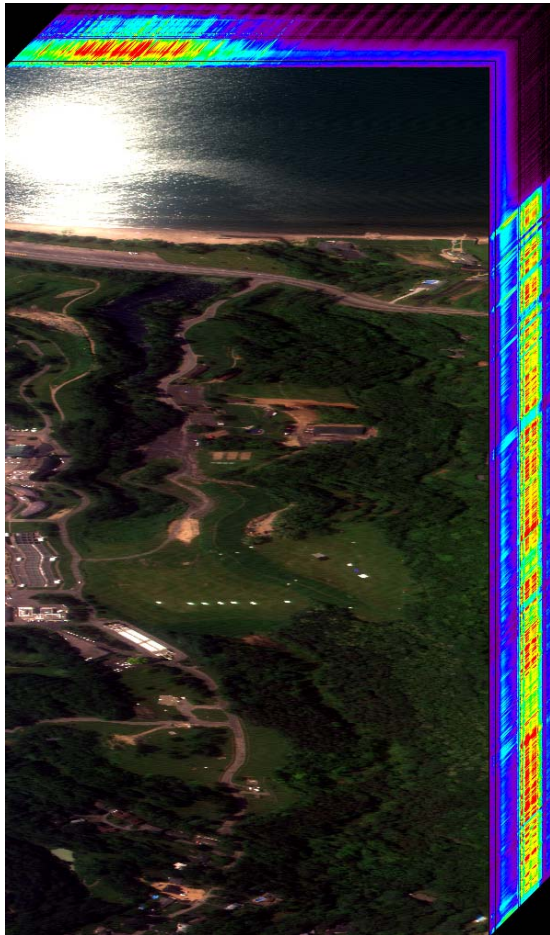


Figure 6: Hyperspectral image cube taken by RIT's MISI sensor for the Megacollect [5].

hyperspectral image cube taken of the area containing the targets by Rochester Institute of Technology's MISI sensor. This representation is just a visualization method. The image shown is a combination of three of the bands in the visual region approximately at the red, green, and blue wavelengths. The cube behind the image represents all of the other band images that were taken by the sensor. In MISI's case, there should be 72 images lined up. These hyperspectral images are part of the data that is input into the MaxD program.

MaxD has various inputs and parameters. The necessary inputs include the target spectral reflectance (in ENVI spectral library format), the target spectral reflectance ENVI header, the MODTRAN generated look-up table based on the image, the image itself, and the image ENVI header [1]. MaxD also has many parameters that can be adjusted to obtain the best results. These include the number of target basis vectors, the number of background basis vectors, and the detection threshold. After making sure that the results from the previously run AVIRIS data can be easily repeated, the first part of the study involved characterizing these various parameters. The data from both MISI and COMPASS was run with

various parameter changes in order to see how varying these parameters affected the results. This procedure was only run for the clean target from the AVIRIS data.

The parameter characterization study will essentially allow researchers to determine whether or not the Invariant Algorithm (implemented in the MaxD program) is a successful and reliable method for contaminated and concealed target detection. The MISI and COMPASS data was tested in MaxD with various parameters. The results were probability maps, which show the probability that the pixel corresponds to the target. Each parameter was adjusted and run. The resulting probability maps are the data that were analyzed and interpreted. Each probability map was evaluated to decipher whether or not the correct pixels were detected as targets.

It was possible that the MaxD program will not detect the target pixels from the MISI and COMPASS data. If this was the case, the reason for its failure must be ascertained. Further

parameter studies were performed, to determine whether adjusting the parameters affected the outcome of the study.

If the Invariant Algorithm implemented in the MaxD program proved to be successful in detecting contaminated and partially concealed targets, numerous revolutionary advances could be made in the practical applications of target detection. This study could be the basis of deciding whether the Invariant Algorithm is reliable for this purpose. Its conclusions will help further the latest developments in the implementation of hyperspectral imagery.

Results

The first step in completing the experiment was to duplicate the results of the previous MaxD test. Figure 1(a) shows the AVIRIS data that was analyzed by Emmett Ientilucci. By using the default values for the parameters (8 MaxD vectors and 2 FSR vectors) and merely adjusting the thresholding, the previously determined results were easily reproduced. Because of the success of this part of the experiment, the next part of the project, the parametric sensitivity study, was begun.

For the second portion of my research, a parametric sensitivity study was completed to determine the ideal parameter values for maximum target detection and minimal false alarms in the AVIRIS image shown previously. The two main parameters that were varied were the number of MaxD vectors and the number of FSR (forward stepwise regression) vectors. The number of MaxD vectors is an estimate of the number of dimensions that the user believes the data lie in. The general consensus before this test was run was that increasing the number of dimensions would achieve better results to a point. It was believed that once a certain number of dimensions were reached, the results would plateau. The number of FSR vectors describes how many of the MaxD vectors the user believes to be linearly independent. This determines the number of target basis vectors to be used. This means that if the user chooses to use three FSR vectors (the default value), the MaxD program will choose three vectors to compare each pixel to.

The first parametric sensitivity that was run involved keeping a constant number of MaxD vectors and varying the number of FSR vectors. Thirty MaxD vectors were used, and the number of FSR vectors was from one to 25 in increments of one. For each run, the target pixel value was recorded (found using the Cursor/Location Value tool in ENVI). To find the number of false alarms, the probability map from each run was opened in ENVI, and the Interactive Stretching function was used to linearly stretch the function with a chosen minimum and maximum value. The minimum was set to the target pixel value, so that only the pixels with values above the target pixel value are shown. ENVI's Interactive Stretching Function displays this percentage of pixels below the minimum pixel value (see Figure 7).

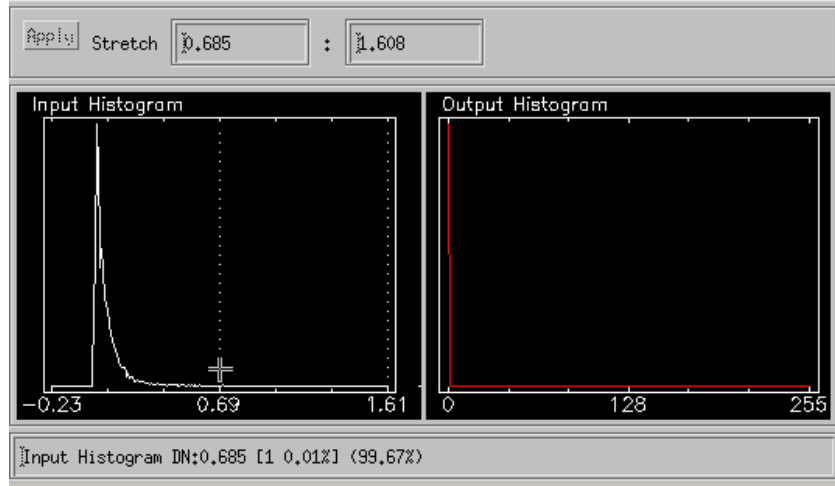


Figure 7: ENVI's Interactive Stretching Function. The number 0.685 is the minimum pixel value (set to the target pixel value), and the 99.67% gives the percentage of pixels below that value.

To find the number of false alarms, the percentage of pixels below the target pixel value was multiplied by the number of pixels in the image (10,000, since the image is 100 by 100 pixels). This number is subtracted from 10,000, since the percentage given was pixel values below the target pixel value. The resulting value is the number of pixels above the target pixel value, or the number of false alarms. This was performed for each run. Figure 19 in the Appendix shows all of the results.

Figures 8(a) and 8(b) were created to aid in the visual interpretation of the results. Figure 8(a) is a plot of the target pixel value versus the number of FSR vectors. This plot shows some very interesting results. Instead of the linear plot that had been hoped for, a random plot was generated. There was no particular trend in the results. There were high pixel values with a low number of FSR vectors (one), a high number of FSR vectors (25), and an intermediate number of FSR vectors (fifteen and seventeen). These are all circled in red. The rest of the runs had very low pixel values, all below 20. Figure 8(b) shows the number of false alarms in the image versus the number of FSR vectors. The points circled in red correspond to the circled pixels in figure 8(a). The plots show that all of the runs with high resulting target pixel values had zero false alarms. This relationship makes logical sense; the higher the pixel value, the less likely that a background pixel has a higher value. There were other runs that had low target pixel values and zero false alarms, but the probability of this combination is lower than that of high pixel value and zero false alarms.

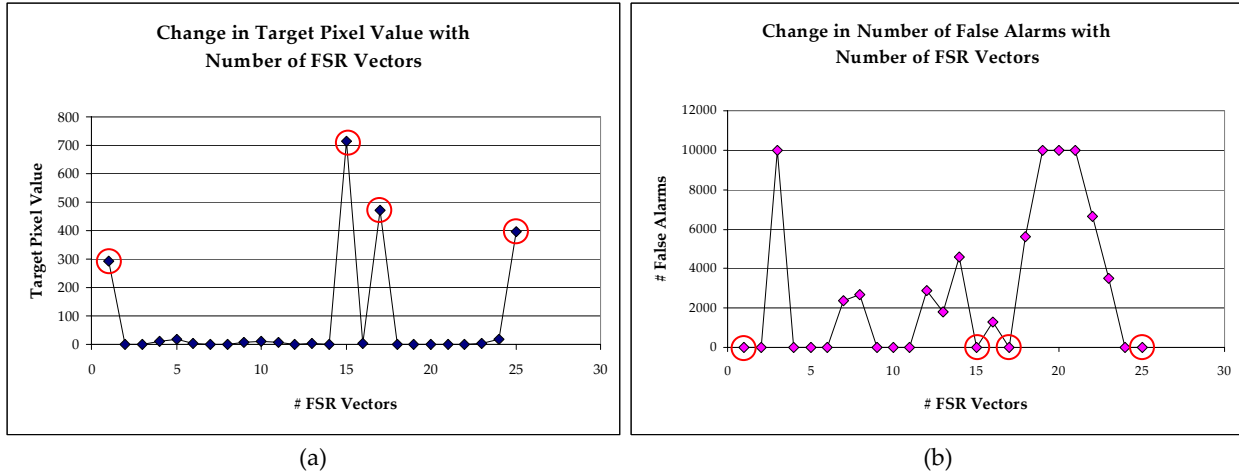


Figure 8: (a) This plot shows the target pixel value versus the number of forward stepwise regression vectors in increments of one. (b) This shows the number of false alarms versus the number of forward stepwise regression vectors in increments of one.

Figures 9(a) and 9(b) show examples of resulting probability maps with varying numbers of FSR vectors. Figure 9(a) shows the complete and zoomed in probability map of the image when 15 FSR vectors were used. The complete probability map clearly illustrates that the target pixel has the highest pixel value. Figure 9(b), however, demonstrates a very low target pixel value, and a high number of false alarms. This figure is the complete and zoomed in probability map of the image when 14 FSR vectors were used. Figure 8(b) shows that for this number of FSR vectors, about 50% of the pixels are false alarms. This means that the target pixel value was actually the lowest value in the image. Surprisingly, as can be seen in figure 8(b), there were a few instances where this was the case. When performing this experiment, there was some confusion as to which pixel to use as the target pixel. Figure 10(a) shows the full true-color image and the image zoomed in so that the target pixel is centered. Figure 10(b) shows a probability map (created using 1 FSR vector) and the zoomed in map. It's clear that this pixel does not appear to be a target pixel. The target in this particular situation is a red basketball court. The "target pixel" is not red at all in the true color image. The explanation for this is that MaxD is a sub-pixel detection algorithm, meaning that it detects pixels that contain both target and background. It seems that this pixel must be a sub-pixel. The pixels that appear to actually be targets do not often have pixel values any higher than the pixel that in this case is considered the target pixel. In fact, the pixel value on the probability map corresponding to the red pixels is very low, as can be seen in figure 10(b). Even when the target pixel value on the probability map is very low, such as in figure 9(b), the pixel values that are red on the corresponding true color image still have very low pixel values. Therefore it is believed that the target pixel found by MaxD in these instances is indeed a mixed pixel, and that it was properly detected.

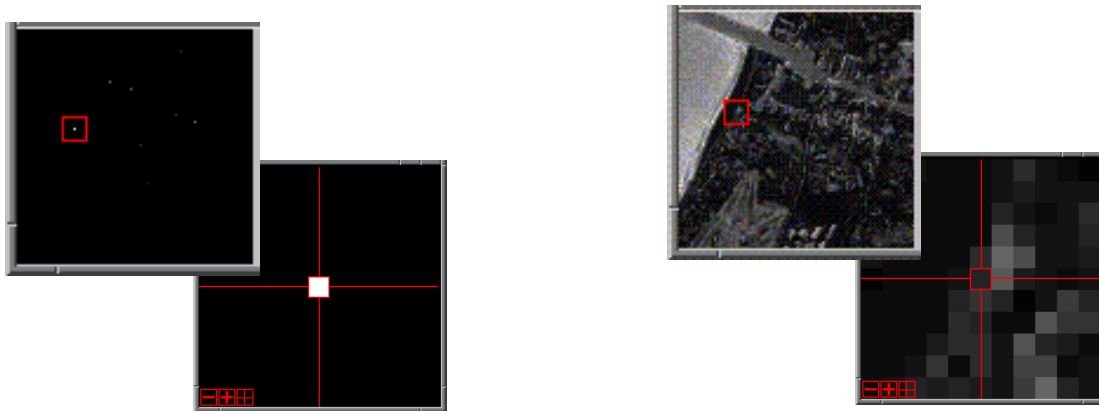


Figure 9: (a) Probability map and target pixel resulting with the use of 15 FSR vectors, where the target pixel has the highest value. (b) Probability map and target pixel resulting with the use of 14 FSR vectors, where the target pixel has the lowest value.



Figure 10: (a) True color image zoomed into what was considered the target pixel. (b) The probability map and target pixel resulting with the use of 25 FSR vectors.

Overall, it seems that the optimal number of FSR vectors is random. In order to find the ideal number of FSR vectors, a similar test must be performed for every different image. For this image, the best number of FSR vectors (in combination with 30 MaxD vectors) is 15 vectors. This will also vary with a change in the number of MaxD vectors specified.

The second parameter that was varied was the number of MaxD vectors. The number of FSR vectors remained constant (the default value of 3), and the number of MaxD vectors varied from 5 to 45 in increments of 5. The results of this study were somewhat counterintuitive. It was found that any number of MaxD vectors greater than 25 produced equal target pixel values and equal (very high) numbers of false alarms. This can be seen in figures 11(a) and 11(b).

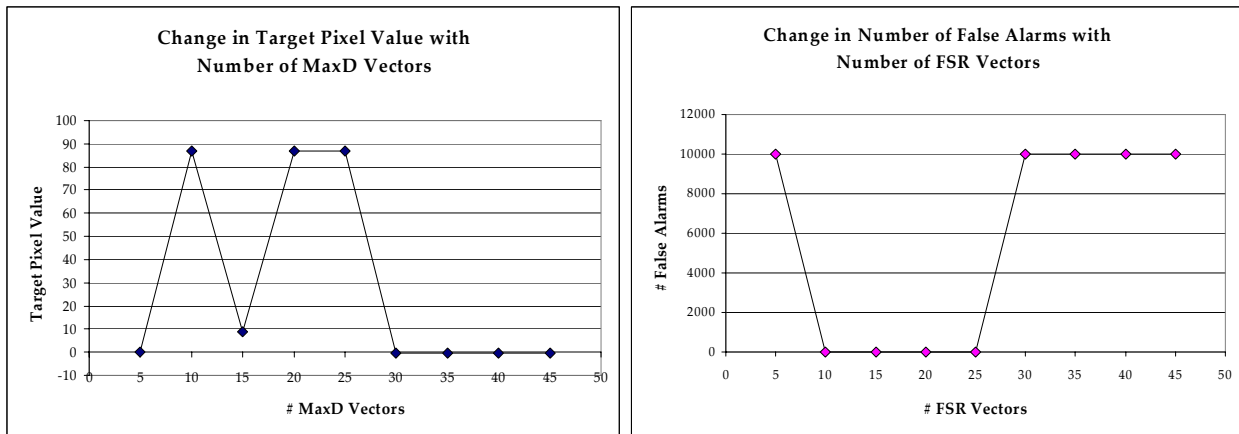


Figure 11: (a) Plot showing the change in the target pixel values with varying numbers of MaxD vectors (in increments of 5) and a constant number of FSR vectors (the default value, 3). (b) Plot showing the change in the number of false alarms for the same parameters.

In this case, all of the runs with target pixel values above zero had zero false alarms, and all of the runs with target pixel values below zero had almost 100% false alarms. This leads to the conclusion that too many MaxD vectors can degrade the performance of the algorithm. For this data, anything over 25 is unnecessary.

The second part of the project involved testing whether or not the Invariant Algorithm (implemented by MaxD) is successful in detecting contaminated and concealed targets. The data that was used for this portion of the project was taken from the June 7th, 2004 Megacollect over Camp Eastman. Figure 12(a) shows the true color MISI image that was used.

Before attempting to detect contaminated and concealed targets, it was necessary to be sure that MaxD detected the clean targets in this image. The target that was used was the gray tarp, centered in the red box in both figures. The image was run with 8 MaxD vectors and 6 FSR vectors. Fewer vectors are required here due to the “lower” complexity of the scene. The linearly enhanced probability map from this run can be seen in figure 12(b). The circled areas on figures 12(a) and 12(b) match up. These areas are regions with high numbers of false alarms.



Figure 12: (a) The true-color MISI image used for testing the effectiveness of MaxD and the Invariant Algorithm on concealed and contaminated targets. (b) Resulting probability map with circled areas of high false alarms.

Unfortunately, there were a great number of false alarms. In figure 12(b), the target pixel has such a low value that it can hardly be seen. Many areas had false alarms with much higher pixel values than the target. There exists, however, a reasonable explanation for these false alarms. Figure 13 shows the reflectance spectrum of the target pixel (the tarp), the shadow in circled section 2 (dark blue), and the dirt in circled section 4 (blue-green). The reflectance spectra are obviously all very similar. The rationalization is that the spectral shapes of these pixels were more similar to the target basis set than the background basis set, and therefore, by the GLRT detection scheme, they have a higher probability of being targets. This demonstrates a limitation of the Invariant Algorithm for target detection.

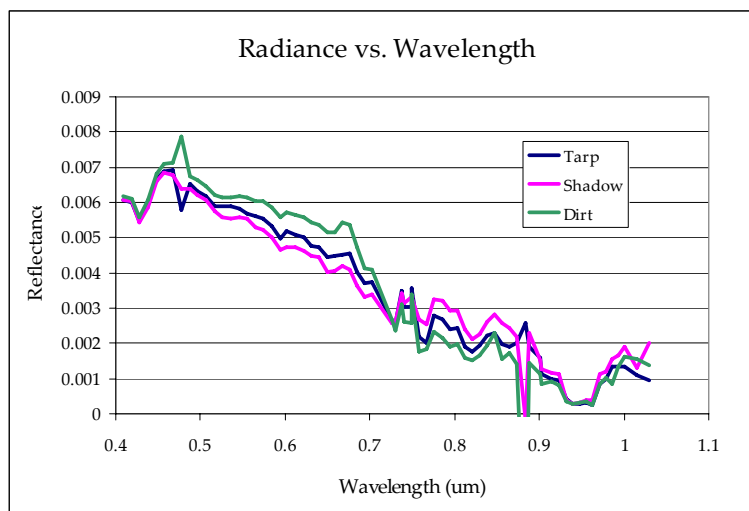


Figure 13: Radiance spectrum of the target (the tarp), and two of the main types of false alarms (shadow and dirt)

MaxD was able to successfully detect the clean targets. Even though there were a great number of false alarms, the next part of the project could be started. Detection of the contaminated target in figure 5(a) was the next goal. This gray tarp was covered with a layer of dirt. During the collect, an Analytical Spectral Device was used to measure the contaminant spectrum as a standard (the ASD measures the spectral reflectance curve from .35 to 2.5 um). The plot of the spectral curve can be seen in Figure 20 in the Appendix. Figure 14 shows the GUI (graphical user interface) opened in MaxD for the construction of the target vectors. The fifth space is the place to input the spectrum of the contaminant (in the ENVI spectral library format). This is an optional input. In this experiment, the spectral curve of the dirt (converted into ENVI spectral library format) was used as the contaminant data. When MaxD is assigning target basis vectors with contaminant data, it implements equation 2, shown below:

$$\rho'_i(\lambda) = (1 - \alpha)\rho_i(\lambda) + \alpha\rho_c(\lambda) \quad (2)$$

Where $\rho'_i(\lambda)$ is the new target reflectance spectrum (combined with contaminant), α is the contaminant level variable, $\rho_i(\lambda)$ is the clean target spectrum, and $\rho_c(\lambda)$ is the contaminant reflectance spectrum. MaxD essentially linearly combines the target basis vectors by the contaminant spectrum, and compares each pixel in the image to the resulting spectrum. The contaminant variable α varies from 0 to .75 and has ten values. The combined target reflectance spectrum $\rho'_i(\lambda)$ has ten different values, one for each value of α .

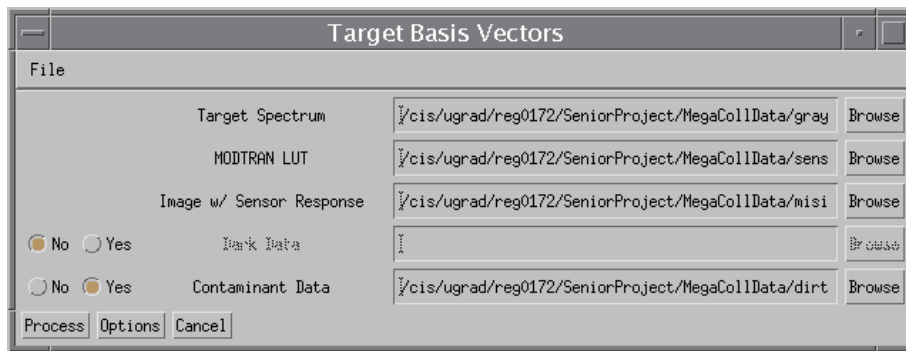


Figure 14: GUI opened in MaxD to construct the target basis vectors including the contaminant data

Unfortunately, MaxD did not find the contaminated target. Figures 15(a)-(c) show the original image zoomed in to the clean targets (circled in blue) and the contaminated target (circled in red), as well as two probability maps zoomed in the same amount.



Figure 15: (a) Original true-color image zoomed in on the clean targets (circled in red) and the contaminated targets (circled in blue). (b) & (c) Probability maps zoomed in on the clean targets and the contaminated targets (also circled in red and blue respectively). The first was created using the default parameter values (8 MaxD vectors and 3 FSR vectors) and the second was created using the parameters found to be ideal for the AVIRIS data (30 MaxD vectors and 15 FSR vectors).

The probability map in figure 15(b) was generated using the default parameter values (8 MaxD vectors and 3 FSR vectors). The probability map in figure 15(c) was generated using the ideal parameter values found in the parametric sensitivity study for the AVIRIS data (30 MaxD vectors and 15 FSR vectors). MaxD clearly did not detect the contaminated targets very well. It was interesting, however, to observe the differences between the two runs. The run with the default parameter values resulted in a target pixel value of 0.634 and 56,016 false alarms (35.01% of the 160,000 pixel image). The run with the best parameter values from the AVIRIS data resulted in a target pixel value of 4.953 and 24,432 false alarms (15.27% of the pixels). The higher number of MaxD and FSR vectors produced fewer false alarms. In order to fully test the contaminated image, a similar parametric sensitivity study must be performed on the image.

Even though the change in parameters had an effect on the number of false alarms in the image, the number is still very high. It is theorized that MaxD failed in detecting the contaminated target because of the lack of a unique spectral shape in the combined target and contaminant curve. Figure 16 shows the spectral curves of the dirt contaminant and the target tarp at a wavelength range of .35 to 2.5um. MISI only records bands from .44 to 1.020um. Figure 17 shows the spectral curves of the dirt contaminant and the target tarp for this smaller range.

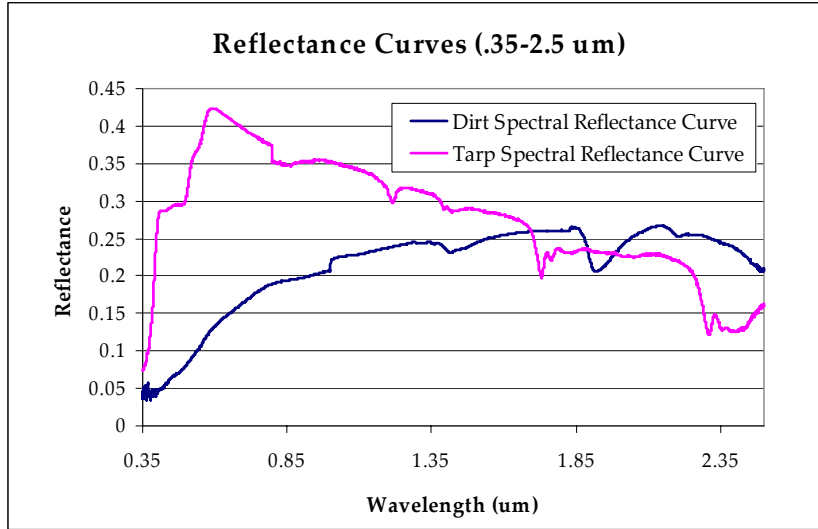


Figure 16: Plot of the reflectance spectral curves of the dirt contaminant and the target tarp for a larger range of wavelengths (.35 to 2.5um).

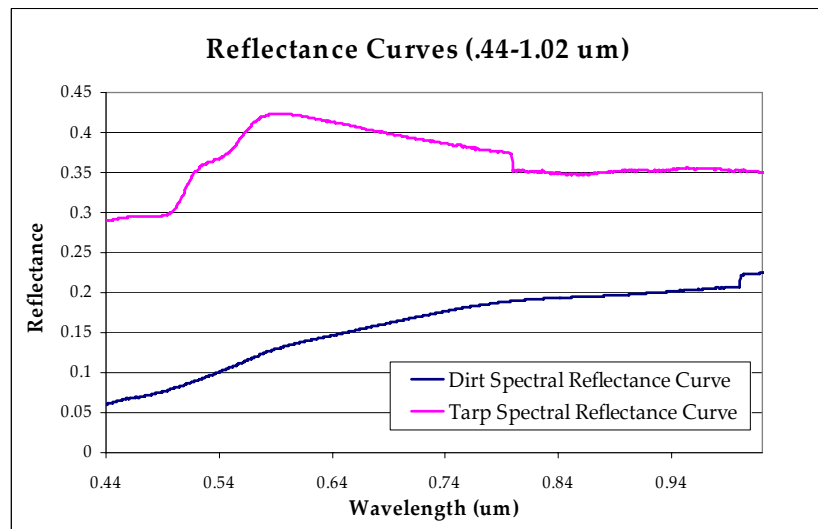


Figure 17: Plot of the reflectance spectral curves of the dirt contaminant and the target tarp in the range that RIT's MISI sensor can record (.44 to 1.020um).

Figure 16 shows the very distinctive differences between the dirt and tarp spectra. Their various peaks and valleys, when combined, would create a very unique new spectral curve for MaxD to search for throughout the image. If the two curves in figure 17 were combined, however, they would not create a very unique spectral curve. The curve of the dirt is essentially just a fairly flat and even line. Combining it with the tarp's spectral curve in this small range would just decrease the reflectance curve of the tarp without changing its actual shape. It is believed that because the shape does not particularly change in this small range of wavelengths, the curve is not unique enough to be detected as the contaminated targets. They simply look like the clean tarp. This theory is supported by the probability maps shown in figures 15(b) and

15(c). The clean target is detected much more successfully than the contaminated target in both runs. According to the proposed theory, this is because the contaminant curve and the target curve, when combined in the range that MISI records, create a curve that looks extremely similar to the original target curve, and therefore only the original target curve is detected.

A similar experiment was performed for the concealed target shown in figure 5(b), which was placed underneath a large, leafy tree. Unfortunately, this target was far too concealed by the tree shadowing it that it could not be detected at all. Instead, the tarp concealed by camouflage net was tested (figures 5(c) and 5(d)). The measured tarp reflectance spectrum can be seen in Figure 21 in the Appendix. The same problem arose as with the contaminated target detection test: the program detected the clean targets far more than the concealed targets. Figure 18(a) shows the zoomed-in true-color MISI image used in the experiment, with the clean targets circled in red and the concealed target circled in blue. Figures 18(b) & (c) show the zoomed-in probability maps generated by MaxD.

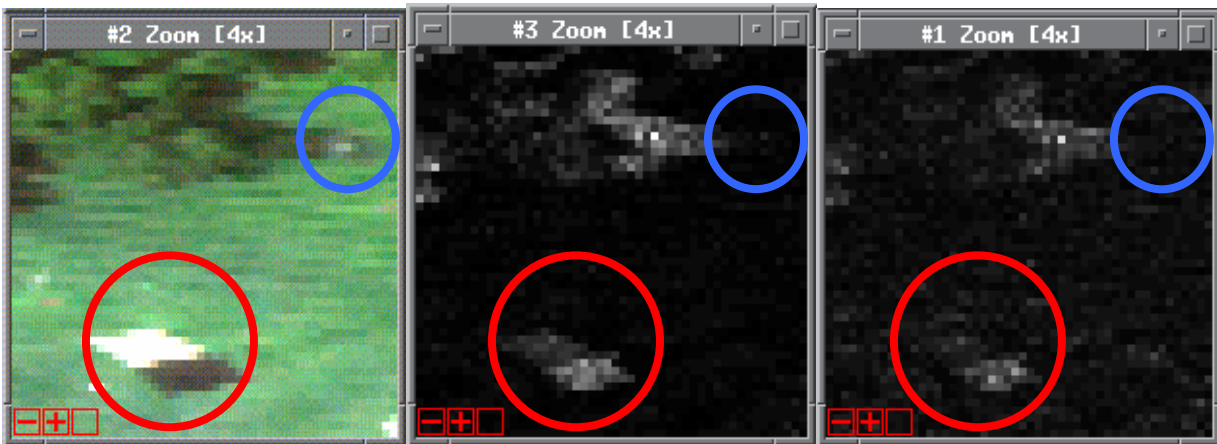


Figure 18: (a) Original true-color image zoomed in on the clean targets (circled in red) and the concealed targets (circled in blue). (b) & (c) Probability maps zoomed in on the clean targets and the concealed targets (also circled in red and blue respectively). The first was created using the default parameter values (8 MaxD vectors and 3 FSR vectors) and the second was created using the parameters found to be ideal for the AVIRIS data (30 MaxD vectors and 15 FSR vectors).

MaxD clearly does not detect this concealed target. It detects the shadowy area to the left of the concealed target in the image, and it detects the clean target. This agrees with the theory presented above, since the shadowy area, as shown in figure 13, has a spectral curve that is very similar to that of the clean tarp.

Two of the probability maps are shown above in figures 18(b) & (c). Figure (b) is the probability map generated by MaxD with the default parameter values (8 MaxD vectors and 3 FSR vectors). The target pixel value for this result was .581, with 59,472 false alarms (37.17% of the 160,000 pixel image). The second probability map, generated with the ideal parameter values found for the AVIRIS data used above (30 MaxD vectors and 15 FSR vectors), had a target pixel value of 2.697 with 50,128 false alarms (31.33% of the pixels). Neither of these runs had particularly successful results. As stated above, it is believed that the lack of success can be attributed to the same problem: that the combination of contaminant and target does not give a

unique enough spectral curve to be detected by MaxD as anything but the target (or shadow and dirt). Further testing is required using data with a higher range of wavelength bands.

Conclusions & Future Work

The results of this study, while not overall successful, provided a very good general understanding of the successes and limitations of the Invariant Algorithm for target detection. Each part of the project led to unique conclusions about the methodology used in the implementation of the algorithm.

The parametric sensitivity study led to multiple useful conclusions. The first conclusion was that an increase in FSR vectors does not necessarily increase or decrease the probability of a target pixel. The relationship is random. This was not an unexpected result. There was hope that the relationship was somewhat linear, and that the higher the number of FSR vectors, the higher the target pixel value (to an extent). The ideal combination of parameters varies for every image. In order to find the ideal number of FSR vectors for an image, a parametric sensitivity test similar to the one performed in this experiment must be completed.

The second conclusion coming out of the parametric sensitivity study was that an increase in FSR vectors does not necessarily increase or decrease the number of false alarms. This relationship is also random. There does seem to be some correlation, however, between target pixel value and the number of false alarms. Intuitively, it makes sense that a higher pixel value corresponds to a lower number of false alarms. This wasn't the case for all runs with low false alarms; some had very low pixel values. But generally, it seems that a high pixel value will lead to a low number of false alarms.

The parametric study led to a third and final conclusion. Although results show a greater sensitivity to the number of FSR vectors than the number of MaxD vectors, the number of MaxD vectors does have an effect on the resulting probability map output by MaxD. Too many MaxD vectors (over 25 in this case) can actually degrade the performance of the MaxD algorithm. To find the maximum number of MaxD vectors before degradation occurs, a test similar to the one performed in this project must be completed.

The second part of the project was not as successful as the parametric sensitivity study, but it still led to useful conclusions. The first component of this part was to test a new set of data from the MISI sensor. This hyperspectral image cube contains data that includes clean, contaminated, and concealed targets. The first step was to attempt to detect the clean targets. This proved successful, but with many false alarms. It became understood that the false alarms were generally pixels that were either in shadow or dirt. The spectral curves of the tarp, dirt, and shadow are all extremely similar. All have very low reflectivity. The sensor detects mostly the contribution of the upwelling radiance. This type of false alarm is inevitable with usual tarps that are used. If a more reflective tarp was used, this problem would probably not transpire.

The next step was to attempt to detect the contaminated target in the scene. MaxD was not considered successful for detecting this target. The assumption for the failure is that the MISI data does not cover a wide enough range of spectral bands to create a unique enough spectral signature for MaxD to detect when the contaminant and the target are combined. A future experiment could be performed to more accurately test MaxD's ability to detect

contaminated targets. This experiment could involve a few different modifications to the present experiment. First of all, a sensor that measures a wider range of wavelength bands could be used, such as COMPASS. There is COMPASS data from the Megacollect, but it is not yet able to be used. Once this data is ready for use, it should be tested with the Invariant Algorithm. If this data is not ready for use, a new set of data could be created with targets and contaminants that have greater differences in spectral curve shape at the shorter wavelengths that MISI can record.

The concealed target study ended up with similar results. MaxD did not detect the targets concealed with a camouflage net, most likely for the same reason that it did not detect the target contaminated by dirt: the MISI data does not cover a wide enough range of spectral bands to create a unique enough spectral signature for MaxD to detect when the contaminant and target are combined. Similar experiments (with either COMPASS data from the Megacollect or new data with greater differences in spectral curve shape at the shorter wavelength bands between the targets and the contaminants) should be performed to properly test MaxD and the Invariant Algorithm on concealed targets.

Most of the sources of error in this experiment were human faults. The MaxD algorithm was run many times, and it is possible that one of the inputs was incorrect. The number of times that the code was run would make a simple mistake like this inconsequential. Another source of error would be the code itself. As the code was first being tested on the AVIRIS data, many bugs were found in the code. It is possible, although very highly unlikely, that an error in the code could account for the algorithm's inability to detect contaminated and concealed targets. It is much more likely, however, that these problems have nothing to do with the code, and more are the fault of the spectral properties of the target and contaminant.

Overall, this experiment was fairly successful in analyzing the performance of the Invariant Algorithm for target detection in hyperspectral imaging. With the knowledge gained from this project, the experiment could be easily reproduced using hyperspectral images from my different kinds of hyperspectral sensors. Further research

References

- [1] Emmett J. Ientilucci, "Using MaxD target detection (MaxDTD) algorithm in ENVI with AVIRIS data," 2004, *Personal Communication*
- [2] D. Manolakis, D. Marden, and G. Shaw, "Hyperspectral image processing for automatic target detection applications," *Lincoln Library Journal*, vol. 14, no. 1, pp. 79-116, 2003
- [3] David Messinger, "Target detection in hyperspectral imagery: the invariant method," 2004, *Personal Communication*
- [4] Bea Thai and Glenn Healey, "Invariant Subpixel Material Detection in Hyperspectral Imagery," *IEEE Transactions on Geoscience and Remote Sensing*, vol. 40, no. 3, pp. 599-608, March 2002
- [5] David Messinger, "RIT Megacollect," *Powerpoint Presentation*, presented October 8th, 2004
- [6] Kris Barcomb, "High Resolution, Slant Angle Scene Generation and Validation of Concealed Targets in DIRSIG," *Masters Thesis*, 2004
- [7] "EOIR Technologies: COMPASS," <http://www.eoir.com/products/compass.htm>

Appendix

# of FSR Vectors	Target Pixel Value	Percent of Pixels below Target Pixel Value	Number of False Alarms
1	291.329175	99.99	9900.01
2	0.681529	99.77	9900.23
3	-0.1407	0.1	9999.9
4	9.329473	99.98	9900.02
5	17.250932	99.99	9900.01
6	2.243184	99.99	9900.01
7	0.982288	76.06	9923.94
8	1.15469	73.1	9926.9
9	6.562763	99.99	9900.01
10	12.287074	99.99	9900.01
11	8.836136	100	9900
12	1.596362	71.27	9928.73
13	2.248778	81.87	9918.13
14	1.14946	54.32	9945.68
15	712.813078	100	9900
16	4.040995	87.3	9912.7
17	472.21606	100	9900
18	0.986584	43.99	9956.01
19	0.061567	0.08	9999.92
20	0.009612	0.09	9999.91
21	-0.040454	0.09	9999.91
22	0.71257	33.71	9966.29
23	2.265911	64.86	9935.14
24	18.534309	100	9900
25	397.335512	100	9900

Figure 19: FSR parametric sensitivity study results

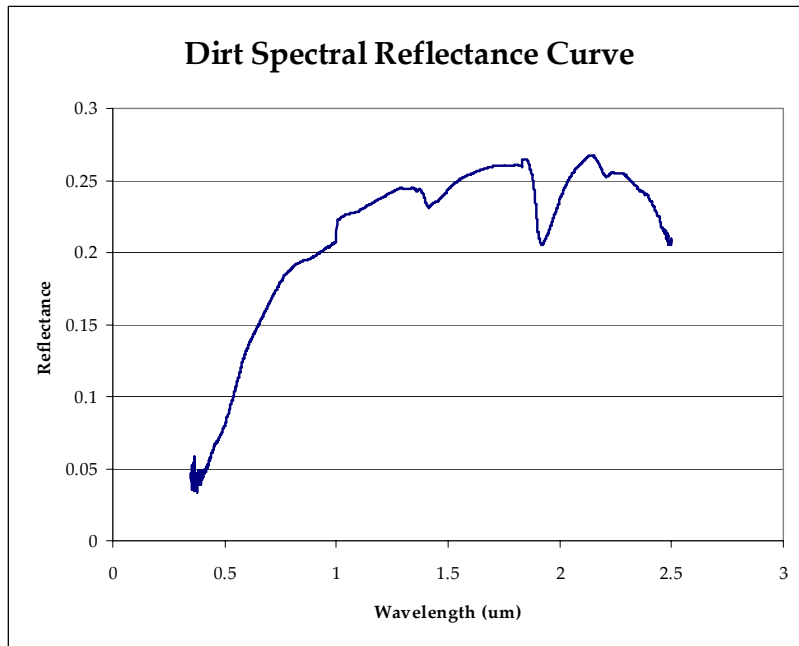


Figure 20: Spectral reflectance curve of the dirt covering the contaminated tarp measured during the Megacollect using the ASD

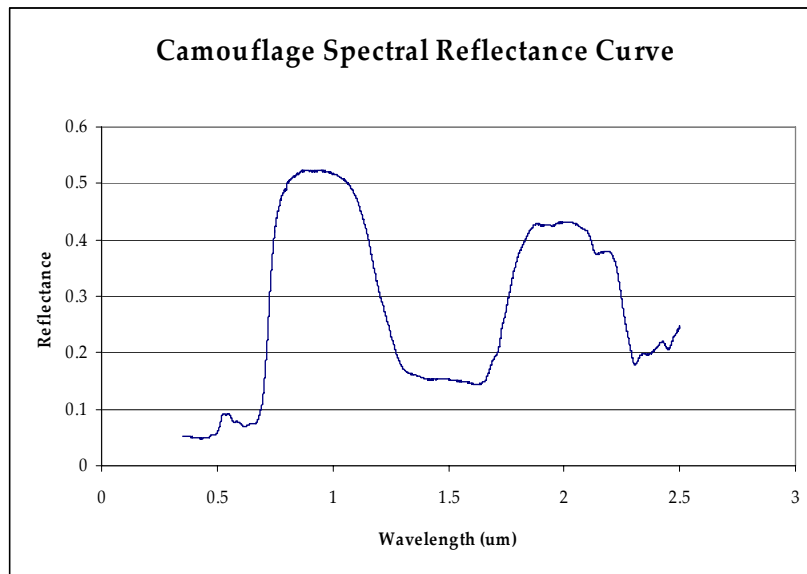


Figure 21: Spectral reflectance curve of the camouflage covering the concealed tarp measured during the Megacollect using the ASD